Facultative endosymbiosis between cellulolytic protists and methanogenic archaea in the gut of the Formosan termite *Coptotermes formosanus*

Masayuki Kaneko[1,‡], Tatsuki Omori[1,‡], Katsura Igai[1], Takako Mabuchi[1], Miho Sakai-Tazawa[1], Arisa Nishihara[2], Kumiko Kihara[1,3],

Tsuyoshi Yoshimura[4,§], Moriya Ohkuma[2], Yuichi Hongoh[1,2,*]

[1]Department of Life Science and Technology, Tokyo Institute of Technology, 2-12-1 Ookayama, Meguro-ku, Tokyo 152-8550, Japan
[2]Japan Collection of Microorganisms, RIKEN BioResource Research Center, Tsukuba, Ibaraki 305-0074, Japan
[3]Department of Biological and Chemical Systems Engineering, National Institute of Technology, Kumamoto College, Yatsushiro, Kumamoto 866-8501, Japan
[4]Innovative Humano-habitability Laboratory, Research Institute for Sustainable Humanosphere, Kyoto University, Uji, Kyoto 611-0011, Japan

[*]Corresponding author: Yuichi Hongoh, Department of Life Science and Technology, Tokyo Institute of Technology, 2-12-1 Ookayama, Meguro-ku, Tokyo 152-8550, Japan. Email: yhongo@bio.titech.ac.jp
[‡]Masayuki Kaneko and Tatsuki Omori should be considered joint first authors.
[§]Tsuyoshi Yoshimura passed away in May 2021.

Abstract

Anaerobic protists frequently harbour methanogenic archaea, which apparently contribute to the hosts' fermentative metabolism by consuming excess H_2. However, the ecological properties of endosymbiotic methanogens remain elusive in many cases. Here we investigated the ecology and genome of the endosymbiotic methanogen of the *Cononympha* protists in the hindgut of the termite *Coptotermes formosanus*. Microscopic and 16S rRNA amplicon sequencing analyses revealed that a single species, designated here "*Candidatus* Methanobrevibacter cononymphae", is associated with both *Cononympha leidyi* and *Cononympha koidzumii* and that its infection rate in *Cononympha* cells varied from 0.0% to 99.8% among termite colonies. Fine-scale network analysis indicated that multiple 16S rRNA sequence variants coexisted within a single host cell and that identical variants were present in both *Cononympha* species and also on the gut wall. Thus, "*Ca*. Methanobrevibacter cononymphae" is a facultative endosymbiont, transmitted vertically with frequent exchanges with the gut environment. Indeed, transmission electron microscopy showed escape or uptake of methanogens from/by a *Cononympha* cell. The genome of "*Ca*. Methanobrevibacter cononymphae" showed features consistent with its facultative lifestyle: i.e., the genome size (2.7 Mbp) comparable to those of free-living relatives; the pseudogenization of the formate dehydrogenase gene *fdhA*, unnecessary within the non-formate-producing host cell; the dependence on abundant acetate in the host cell as an essential carbon source; and the presence of a catalase gene, required for colonization on the microoxic gut wall. Our study revealed a versatile endosymbiosis between the methanogen and protists, which may be a strategy responding to changing conditions in the termite gut.

Graphical abstract
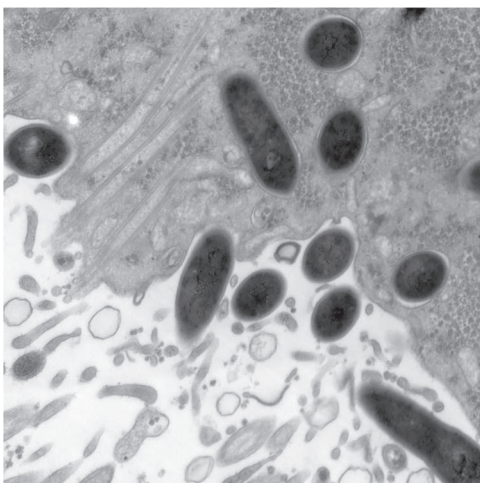
Keywords: symbiosis, endosymbiont, gut microbiome, insect, protozoa, methanogen, Methanobrevibacter

Introduction

Methanogenic archaea, or methanogens, play a key role in the final step of the decomposition of organic matter in various anaerobic environments [1]. In the guts of termites, for example, which are keystone animals in the terrestrial carbon cycle, methanogens accounted for 0%–10% of the prokaryotic gut community and possibly produce 1%–3% of the global methane [2, 3]. Methanogens are present in the guts of diverse termite lineages [4, 5] and are considered to contribute to the gut ecosystem as H_2-sinks by producing methane from H_2 and CO_2 [6, 7]. Methanogens are found on the hindgut epithelium [4, 8, 9] or within the cells of certain gut protist species [10]. The protists in the termite gut belong to the phylum *Parabasalia* or the order *Oxymonadida* in the phylum *Preaxostyla* and play major roles in the digestion of lignocellulose [11]. These gut protists generally harbour endo- or ectosymbiotic prokaryotes, which likely contribute to the host nutrition by supplying nitrogenous compounds [11] and/or removing H_2 [12, 13]. In addition to the mutualistic symbionts, commensal or parasitic endosymbiotic bacteria are occasionally present [14].

Endosymbiotic methanogens are observed, for example, in the parabasalid protist *Trichomitopsis termopsidis* in the gut of the termite *Zootermopsis angusticolis* [15, 16] and the oxymonad protist *Dinenympha parva* in the gut of the termite *Reticulitermes speratus* [17, 18]. It has been hypothesized that endosymbiotic methanogens promote wood decomposition of the protist hosts by consuming excess H_2 [10], but their detailed physiology and ecology remain unclear. Indeed, although there are numerous examples of endosymbiosis between anaerobic protists and methanogens in various environments, the ecological properties of endosymbiotic methanogens, including whether they are obligate or facultative endosymbionts, are elusive in many cases [19, 20].

The Formosan subterranean termite *Coptotermes formosanus* is the most destructive pest of wooden constructions in southern China and Japan and has invaded Hawaii and the southern part of the USA [21]. The termite harbours a relatively simple protistan gut community consisting of five unculturable parabasalid species: *Pseudotrichonympha grassii*, *Holomastigotoides hartmanii*, *Holomastigotoides minor*, *Cononympha* [*Spirotrichonympha*] *leidyi*, and *Cononympha koidzumii* [22–24]. Among them, endosymbiotic methanogens are found only in *Cononympha* cells [25, 26], which are mainly localized in the posterior part of the hindgut [27, 28]. *Cononympha* protists numerically dominate the protistan gut community, occupying 2200–10 900 out of 3800–12 900 total protist cells per gut [28]. Transcriptomic analysis of *Cononympha* cells suggested that *Cononympha* hydrolyzed cellulose, hemicellulose, pectin, and chitin, contributing to both lignocellulose digestion and nitrogen recycling [24].

In the present study, we examined the ecology and metabolic capacity of the uncultured endosymbiotic methanogen of *Cononympha* species in the gut of *C. formosanus* using a combination of microscopy, fine-scale phylogenetic analysis, and genome sequence analysis. Here, we show evidence of facultative endosymbiosis with frequent horizontal acquisitions of the methanogen and its genome features adapted to the lifestyle. Our study sheds light on another aspect of the multilayered symbiotic system in the termite gut.

Materials and Methods
Termite collection and methanogen infection rate

C. formosanus (family Rhinotermitidae) were collected from four prefectures in Japan (Table S1). The termite colonies collected in 2019 or later were kept with their nest logs in plastic containers in a laboratory until use. Colonies collected in 2018 or earlier were kept in laboratories for years fed with red pine chips. The entire guts of three worker termites per colony were removed using sterile forceps, and the gut contents were suspended in sterile solution U [29]. The ratio of methanogen-containing *Cononympha* cells to total *Cononympha* cells in individual guts was examined on the basis of F_{420} autofluorescence under an Olympus BX51 epifluorescence microscope. The procedure of CH_4 measurement emitted by termites and semi-quantitative PCR amplification of the gene for methyl coenzyme M reductase (McrA) are described in Supplemental Methods.

Collection of single *Cononympha* cells and sequencing of 18S rRNA genes

Single *Cononympha* cells were collected using a Leica AM6000 micromanipulation system and subjected to whole genome amplification (WGA) using the illustra GenomiPhi V2 kit (GE Healthcare) as described previously [30]. To identify the species of *Cononympha*, the 18S rRNA gene was amplified by PCR using *Cononympha*-specific primers designed in this study (Table S2). The PCR conditions are described in Supplemental Methods. The PCR products were purified, cloned, and sequenced using the Sanger method as described previously [30].

16S rRNA amplicon sequencing analysis

The V3–V4 region (ca. 400 bp) of the 16S rRNA gene was amplified by PCR with prokaryote-universal primers, Pro341F, and Pro805R (Table S2), using Phusion High-Fidelity DNA Polymerase (New England Biolabs), as described previously [31]. Purification, library preparation, and paired-end sequencing (300 bp × 2) on the MiSeq platform with the MiSeq Reagent Kit v3 (Illumina) were conducted as described previously [31]. The paired-end reads were trimmed, quality filtered, and sorted into amplicon sequence variants (ASVs) using DADA2 v1.6 [32]. The ASVs were classified using SINA v1.2.11 [33] with the SILVA v132 database [34]. ASVs classified as *Eukarya* or undetermined and ASVs of which frequency was <0.1% of the total reads were discarded from subsequent analyses.

Phylogenetic analysis of 16S rRNA genes

Near full-length 16S rRNA genes of methanogens were amplified by PCR using Phusion Hi-Fidelity DNA Polymerase. Primers M23F and M1382R broadly targeting methanogens were used for gut wall samples, while primer CfC-M23F adjusted to the sequence of the endosymbiotic methanogen was used as the forward primer for endosymbiotic methanogens (Table S2). The PCR conditions and procedures of sequencing and alignment are described in Supplemental Methods. A maximum-likelihood tree was constructed using IQ-TREE v1.6.12 [35] with the $TVM + F + I + G4$ nucleotide substitution model selected by ModelFinder implemented in IQ-TREE. Network construction of sequence variants (SVs) was conducted using the PopART program depending on Qt v4.8.5 with TCS algorithms [36].

Fluorescence in situ hybridization and transmission electron microscopy

To discriminate between *Con. leidyi* and *Con. koidzumii* cells, oligonucleotide probes specific to each 18S rRNA sequence were designed using ARB [37] (Table S2). Fluorescence in situ hybridization (FISH) was performed as described previously [38] with hybridization at 55°C for 2 h. Observations were conducted under the Olympus BX51 epifluorescence microscope.

Transmission electron microscopy (TEM) was performed as described previously [39] using an H-7500 transmission electron microscope (Hitachi).

Genome sequencing

Single *Cononympha* cells were collected as described above, washed several times in droplets of solution U, and transferred to solution U containing 0.1% Tween 20 (Nacalai Tesque). Prokaryotic cells that leaked out from the ruptured host cell were collected with a glass capillary attached to the Leica AM6000 micromanipulation system and subjected to WGA as described above. Nine WGA samples of single *Cononympha* cells were prepared. These were subjected to paired-end sequencing on the MiSeq platform. After assembling and binning as below, one sample was selected for deeper paired-end sequencing and mate-pair sequencing on MiSeq, and long-read sequencing on the MinION platform (Oxford Nanopore Technologies), based on the estimated genome completeness of the target methanogen. The procedures for library preparation and sequencing are described in Supplemental Methods.

Genome assembly

The MiSeq paired-end reads were trimmed, quality filtered, and assembled into contigs using SPAdes v3.9 [40]. The contigs were binned using a combination of MyCC [41] and Contig Annotation Tool (CAT) [42]. The results were evaluated for the selection of the best sample. The MinION reads, after being quality trimmed, were assembled together with the quality-trimmed MiSeq paired-end and mate-pair reads into contigs using SPAdes v3.15.2 with the "hybrid-assembly" and "meta" mode [40]. The assembled contigs ≥500 bp were binned using a combination of MyCC, CAT, RAST (http://rast.nmpdr.org/rast.cgi), and BLASTn searches. The bin affiliated with *Methanobrevibacter* was further subjected to scaffolding using LINKS v2.0.1 [43] and gap-closing using TGS-GapCloser [44]. The quality-trimmed MiSeq and MinION reads were mapped onto the gap-closed bin using BBMap v38.96 and Minimap2 v2.24-r1122 [45]. The reads mapped onto the bin were then reassembled using SPAdes v3.15.2 with the "hybrid-assembly" and "sc" mode. Reassembled contigs ≥1000 bp were binned as described above. Details of quality filtering are described in Supplemental Methods.

Gene annotation

Finding and functional annotation of genes were performed using a combination of DFAST [46] and BLASTp searches of the NCBI non-redundant (nr) protein database. CRISPR-Cas systems were identified using CRISPRCasFinder [47]. Assignment of COG (clusters of orthologous genes) categories [48] was conducted by RPS-BLAST v2.6.0+ searches of the NCBI Conserved Domain Database v3.16, and the results were manually curated. Pseudogenes were manually identified as described previously [49]. Metabolic pathways were inferred using the KEGG automatic annotation server (KAAS) [50] and KEGG Mapper [51].

Phylogenomics

To construct a phylogenomic tree, we retrieved genome sequences of *Methanobacteriaceae* as references from GTDB r202 [52] and metagenome-assembled genomes (MAGs) assigned to *Methanobacteriaceae* recently obtained from termite guts [5, 53]. Gene prediction, extraction, and alignment are described in Supplemental Methods. A maximum-likelihood tree was constructed using IQ-TREE v1.6.12 with the LG + F + R5 amino acid substitution model selected by ModelFinder. The robustness of the tree topology was evaluated using 1000 ultrafast bootstrap resamplings. Average nucleotide identity (ANI) and average amino acid identity (AAI) were calculated using ANI/AAI-Matrix [54].

Comparative genome analysis

The relative abundance of genes assigned to COG functional categories was calculated for genome sequences with >80% estimated completeness (Table S3). Principal component analysis was performed after a central log-ratio transformation using a script (https://github.com/dkato2021/COGplot.git). To compare genome contents with an identical criterion, the identification of intact genes or pseudogenes was automatically performed using Pseudofinder v1.1.0 [55] and the NCBI Prokaryotic Genome Annotation Pipeline (PGAP) [48].

Results

Discovery of *Cononympha* cells lacking endosymbiotic methanogens

During our preliminary observations of protists in the guts of *C. formosanus* by epifluorescence microscopy, we unexpectedly found that, in certain *C. formosanus* colonies, no *Cononympha* cells emitted F_{420} autofluorescence as a characteristic signal of the presence of endosymbiotic methanogens, unlike in other *C. formosanus* colonies (Fig. 1A–D) or previous reports [25, 26, 28]. To confirm the absence of methanogens in *Cononympha* cells in such termite colonies, we performed amplicon sequencing analysis of the 16S rRNA V3–V4 region for prokaryotic microbiota associated with individual *Cononympha* cells. A total of 30 single *Cononympha* cells collected from two *C. formosanus* colonies (O2020a and O2020b in Table S1), in which almost all *Cononympha* cells were without F_{420} autofluorescence, were examined. For comparison, we also conducted the same experiment using 28 single *Cononympha* cells from two colonies (K2019b and K2019c in Table S1), in which almost all *Cononympha* cells exhibited F_{420} autofluorescence. No 16S rRNA sequences of methanogens were obtained from the former 30 *Cononympha* cells, whereas sequences of *Methanobrevibacter* were recovered from all of the latter 28 *Cononympha* cells (Fig. S1).

Infection rate of methanogens in *Cononympha* cells and methane emission rate

We examined the infection rate of methanogens in *Cononympha* cells for 33 colonies of *C. formosanus* collected from four prefectures in Japan (Table S1), based on the detection of F_{420} autofluorescence. The infection rate greatly varied from 0% to 99.8% depending on the termite colonies (Fig. 1E; Tables S1 and S4). This difference was irrespective of natural or laboratory-reared termite colonies and prefectures of the sampling sites (Fig. 1E; Tables S1 and S4).

To test whether the presence or absence of the endosymbiotic methanogens of *Cononympha* is linked to the methane emission rate from the termite hosts, we chose three *C. formosanus* colonies of the high and low endosymbiotic methanogen-infection rate types, respectively (Fig. 1E; Table S1; Supplementary Methods). The results showed that termites from the colonies of the "high infection rate" type emitted 4.5–7.8 times more methane than those from the "low infection rate" type colonies (Fig. 1E). Semi-quantitative PCR targeting the *mcrA* gene in the entire gut microbiota generated results consistent with the methane emission rates (Fig. S2; Supplementary Methods). No *mcrA* amplification was detected in any of the four tested *C. formosanus* colonies of the "low infection rate" type under the PCR condition, where *mcrA*
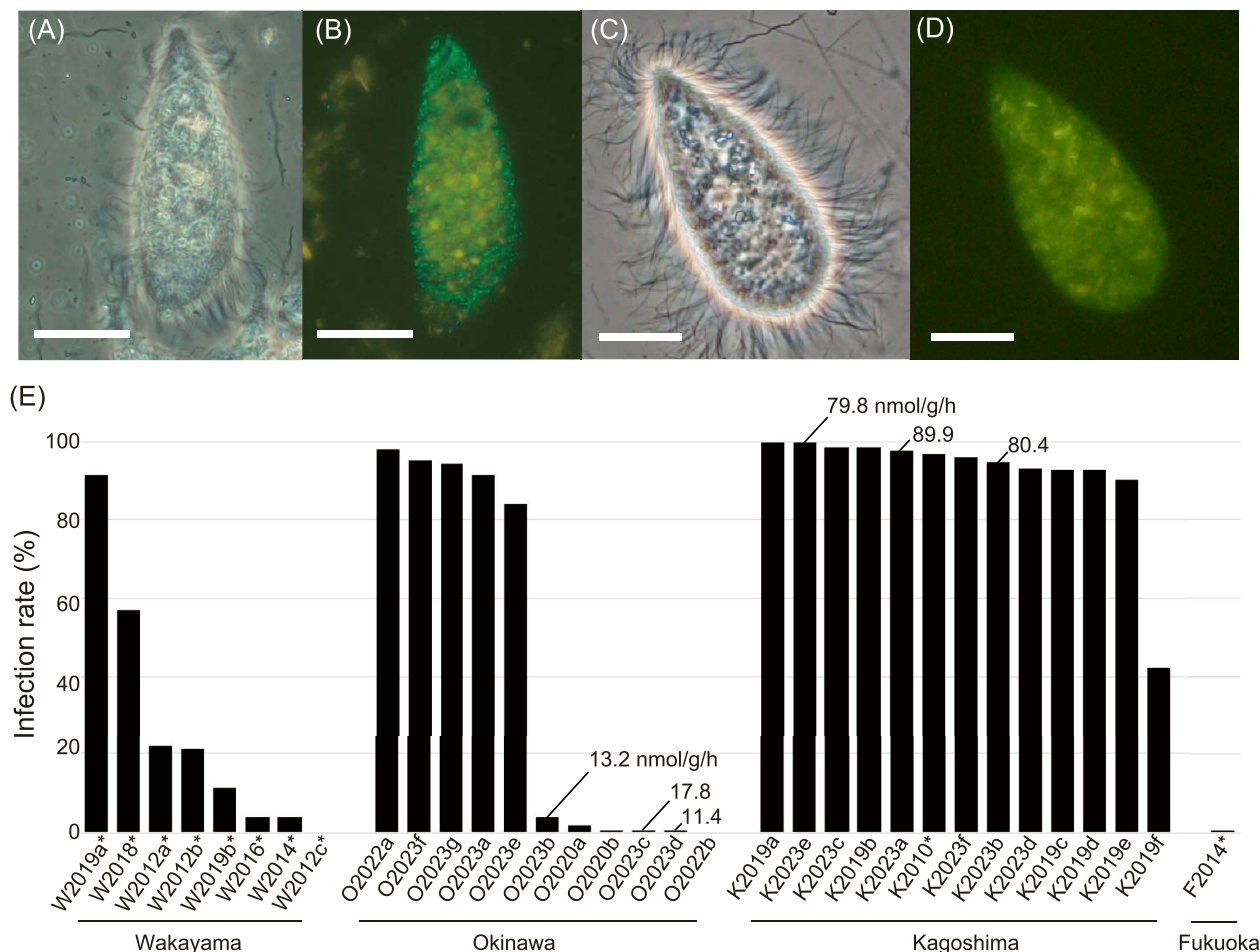
Figure 1. Detection of endosymbiotic methanogens of *Cononympha* protists in the hindgut of *Coptotermes formosanus*. (A, C) Phase-contrast images of *Cononympha* cells. (B, D) Epifluorescent images. Endosymbiotic methanogens are visible with their greenish F_{420} autofluorescence in panel B, whereas no signal was detected in panel D. Amorphous yellow is the autofluorescence of wood particles. Bars indicate 10 μm. (E) Ratio of methanogen-containing *Cononympha* cells to total *Cononympha* cells in individual termite guts across 33 termite colonies. Values indicate methane emission rates (nmol^{-1} g termite^{-1} h^{-1}) averaged between biological replicates. Asterisks attached to termite colony IDs indicate laboratory-reared termite colonies.

amplicons were detected in all six tested colonies of the "high infection rate" type (Fig. S2; Table S1).

Because the hindgut wall of *C. formosanus* can be another habitat of methanogens [56], we examined F_{420} autofluorescence signals on gut wall fragments from termite colonies of both "high infection rate" and "low infection rate" types. We observed dense colonization of rod-shaped methanogens on fragments of the hindgut wall from two out of seven colonies of the "high infection rate" type, whereas almost no signals were detected in termites from four colonies of the "low infection rate" type (Fig. S3; Table S1).

Fine-scale phylogenetic composition and host specificity of endosymbiotic methanogens

In the above 16S rRNA amplicon sequencing analysis (Fig. S1), multiple ASVs belonging to *Methanobrevibacter* were obtained from each *Cononympha* cell (Fig. S4). Nine closely related ASVs were obtained in total, showing only 1–4 mismatches out of 386 bp. Among them, the ASV-3 sequence was identical to the corresponding region of clone SlMeN10 (AB360373), which was derived from *Cononympha* cells in a *C. formosanus* gut [26]. Since the genome of the endosymbiotic methanogen contains only a single rRNA operon as described below, these multiple ASVs were not derived from intragenomic variation. These results indicated that

multiple strains of a single *Methanobrevibacter* species frequently coexisted within a single *Cononympha* cell.

Next, we examined whether both *Cononympha* species, i.e., *Con. leidyi* and *Con. koidzumii*, can harbour methanogens. We obtained the 18S rRNA gene sequences of single *Cononympha* cells used in the above 16S rRNA amplicon analysis (Fig. S1) and found that both *Cononympha* species housed methanogens in colonies of the "high infection rate" type (Fig. S5; Table S5). Conversely, in colonies of the "low infection rate" type, both *Cononympha* species lacked methanogens (Fig. S5; Table S5). We observed that both *Cononympha* species, visually discriminated by FISH specifically targeting 18S rRNA of each species, harboured *Methanobrevibacter*-like rods (Fig. S6).

We further investigated whether the lineages of the endosymbiotic methanogens are distinct, even though closely related, between the two host *Cononympha* species or not. In addition, we examined the phylogenetic relationship between the endosymbionts and the methanogens on the gut wall. To examine these with higher resolution, we obtained near full-length 16S rRNA gene sequences of methanogens by PCR amplification from 14 single *Con. leidyi* cells, three single *Con. koidzumii* cells, and seven fragments of the hindgut wall (Fig. 2; Tables S1 and S5). Three out of four 16S rRNA gene SVs of methanogens associated with *Con. koidzumii* cells were also obtained from *Con. leidyi* cells. In addition,
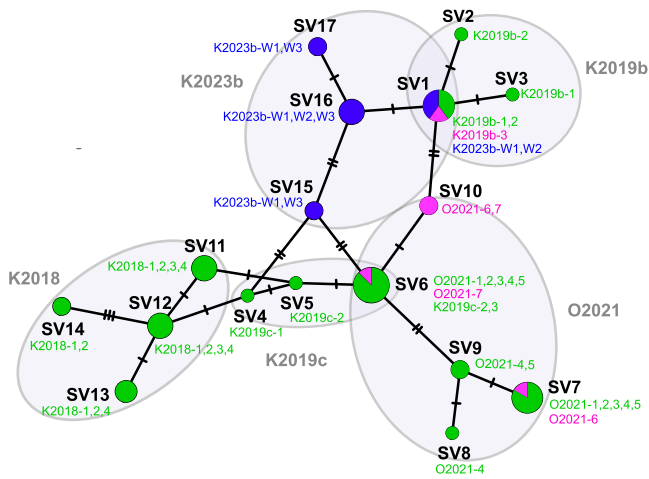
Figure 2. Network analysis of 16S rRNA gene sequence variants (SVs) of methanogens obtained from *Cononympha leidyi* (green), *Cononympha koidzumii* (magenta), and gut wall (blue). Unambiguously aligned 1312 nucleotide sites were used. The circle size of each SV is equivalent to the number of samples of single *Cononympha* cells or gut wall fragments, from which the corresponding SVs were detected. Slashes on branches indicate the number of nucleotide substitutions. The SVs were clustered by termite colonies, and their colony IDs and *Cononympha* cell IDs are shown (see Tables S1 and S5).

we obtained 16S rRNA gene amplicons of methanogens from three of the seven gut wall fragments and sequenced 24 clones in total, all of which showed 99%–100% sequence similarities to SVs of the endosymbionts (Fig. 2). These SVs from the gut wall or *Cononympha* cells formed clusters that were delineated mainly by the host *C. formosanus* colonies (Fig. 2); thus, the sequence variations of these methanogens were strongly related to the host termite colony and not to the *Cononympha* species.

These data together indicated that the endosymbiosis between the *Cononympha* protists and the methanogens is facultative and that the two *Cononympha* species can horizontally acquire the same *Methanobrevibacter* species. Furthermore, the spatial distribution of the methanogen most likely extends to the gut wall of the termite host. The shape and size of the methanogens on the gut wall (Fig. S3A) and within *Cononympha* cells were similar. Both methanogens were straight rods, and the size was 1.1–1.8 μm by 0.4–0.5 μm ($n=50$) in the former while it was 1.3–1.8 μm by 0.4–0.5 μm ($n=50$) in the latter.

TEM of endosymbiotic methanogens

The facultative nature of this endosymbiosis was further corroborated by TEM. An electron micrograph showed that electron-dense, rod-shaped prokaryotic cells, morphologically indistinguishable, were present not only within a *Cononympha* cell but also on its surface (Figs 3 and S7A–D). They appeared to be in the process of phago- or exocytosis by the *Cononympha* cell (Figs 3 and S7A). These prokaryotic cells morphologically resembled cells of cultured *Methanobrevibacter* species [8, 9, 57]. The intracellular ones were surrounded by a host membrane (Figs 3 and S7A–D), and some were localized proximal to putative hydrogenosomes (Figs 3B and S7C). Intracellular *Methanobrevibacter*-like cells apparently during fission were observed (Fig. S7D); they likely proliferate within the host *Cononympha* cell. We hereafter designated this endosymbiotic methanogen as "*Candidatus* Methanobrevibacter cononymphae*" (abbreviated as *Mbv. cononymphae*), and the species description is presented below.
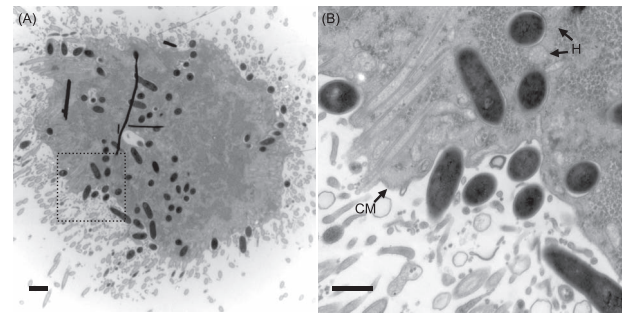
Figure 3. Transmission electron microscopy of a *Cononympha* cell. (A) Section of a *Cononympha* cell. Several black lines are artefacts. (B) Magnified view of the boxed region in panel (A). Electron-dense *Methanobrevibacter*-like cells were observed within the host cytoplasm and also on the host cell surface. H: Examples of putative hydrogenosomes; CM: Cytoplasmic membrane of *Cononympha*. Bars = 1 μm (A); 500 nm (B).

Phylogenetic position of *Mbv. cononymphae* based on 16S rRNA gene

Based on the near full-length 16S rRNA gene, *Mbv. cononymphae* was placed within a clade exclusively comprising uncultured clones derived from termite guts (Fig. S8). Within this clade, *Mbv. cononymphae* was closely related to clones obtained from the protists *Microjoenia* sp. and *D. parva* in the gut of *R. speratus* [17]. This clade further formed a monophyletic cluster with termite-gut-derived sequences, including cultured species inhabiting the gut epithelium of the protist-dependent termite *Reticulitermes flavipes*, i.e., *Methanobrevibacter curvatus* [8] and *Methanobrevibacter filiformis* [9]. Endosymbiotic *Methanobrevibacter* housed by an anaerobic ciliate, *Nyctotherus ovalis*, in the hindgut of the cockroach *Blaptica dubia* [58] and that housed by an aquatic anaerobic ciliate, *Trimyema compressum* [20], were more distantly related (Fig. S8).

General genome features of *Mbv. cononymphae*

We obtained a draft genome sequence of *Mbv. cononymphae* from a single *Cononympha* cell. The genome consisted of 245 contigs with 100% and 98.6% completeness estimated using CheckM [59] and CheckM2 [60], respectively (Table 1). Although only a single rRNA operon was identified in this genome as in many other *Methanobrevibacter* species (Table 1), we recovered four near full-length 16S rRNA gene SVs showing 3–5 base mismatches by PCR amplification from the same DNA sample. Thus, this genome sequence was derived from multiple, at least four, genomovars and here designated as the composite genome "CfCl-M3".

The total contig length was 2 709 899 bp, and 1834 protein-coding sequences (CDSs) were predicted, excluding 90 CDSs truncated by contig ends and 203 CDSs <100 amino acid sequences that were automatically predicted but with no significant hits in BLASTp searches of the NCBI nr protein database. At least, two CRISPR-Cas systems were identified with a total of 282 spacer sequences (Tables S6–S8). Most spacers showed no sequence similarity to those in CRISPRCasdb [61]. The number of pseudogenes was 148 after manual inspection (Table 1), and 14 were assigned to category [V] (defence mechanism) of COGs, including DNA restriction-modification systems and *cas* genes (Fig. S9; Table S6). Finding of duplicated regions and the frequency of single nucleotide polymorphisms in the CfCl-M3 composite genome are described in Supplemental Methods, Supplemental Results, and Table S9.

Table 1. General genome features of "*Ca.* Methanobrevibacter cononymphae" and related species.

species	"*Ca.* Mbv. cononymphae" CfCl-M3	*Mbv. curvatus* (GCA_001639295)	*Mbv. filiformis* (GCA_001639265)	*Mbv. cuticularis* (GCA_001639285)	NOE (GCA_003315655)
Habitat	Intracellular/gut wall	Gut wall	Gut wall	Gut wall	Intracellular
Total length (Mb)	2.71 (2.67[d])	2.41	2.61	2.61	1.91
Contig	244	232	295	169	70
Completeness[a] (%)	98.6	98.2	97.1	99.7	99.3
G + C (%)	27.2	25.7	27.0	26.8	25.3
CDS[b]	2319 (1834)	1883	1985	1869	2175
Coding density (%)[b]	65.8 (59.7)	68.5	68.5	66.2	68.3
rRNA	3	3	3	3	3
tRNA	28	31	30	32	33
Pseudogene[c]	29/174 (148)	11/86	9/83	15/117	95/209 (187)

[a]Estimated using CheckM2 v.1.0.1. [b]Identified using Prodigal v2.6.3. Manually curated values are shown in parentheses. [c]Identified using Pgap/Pseudofinder with those within 1000 bp region from both contig ends being excluded. The number was manually curated for CfCl-M3 in this study and previously for NOE [57] and shown in parenthesis. [d]Total length with duplicated CDSs being excluded.

Phylogenomics and comparative genome analysis

A maximum-likelihood tree based on concatenated amino acid sequences of conserved single-copy genes (Fig. 4; Table S3) was basically congruent with the 16S rRNA gene tree (Fig. S8). *Mbv. cononymphae* belonged to a monophyletic cluster consisting exclusively of MAGs and two *Methanobrevibacter* isolates obtained from the guts of protist-dependent termites. These genomes shared at least 75% ANI and 60% AAI (Fig. S10). This clade was sister to a clade comprising genome sequences from protist-dependent/independent termite guts or other environments (Fig. 4).

Genome sequences derived from termite guts in these two clades (Fig. 4) tended to possess more genes assigned to the COG categories [L] (replication, recombination, and repair) and [V] (defense mechanisms) (Fig. S11). Among the genes, those related to DNA methylation and drug resistance were especially abundant in termite-gut derived genomes (Fig. S12). No clear differences in the number and ratio of genes assigned to respective COG categories were observed among the five *Methanobrevibacter* species in Table 1, except for a much smaller number and ratio of genes assigned to [V] (defense mechanism) in *Methanobrevibacter* sp. NOE (Fig. S13), which is likely an obligate endosymbiont [57].

The number of pseudogenes of *Mbv. cononymphae* was approximately 1.5–2.1 times larger than those of the gut-wall dwelling *Mbv. curvatus*, *Mbv. filiformis*, and *Methanobrevibacter cuticularis*, but smaller (ca. 80%) than that of *Methanobrevibacter* sp. NOE (Table 1). The distribution pattern of pseudogenes among COG categories indicated that pseudogenes were characteristically accumulated in *Mbv. cononymphae* in categories [L] (replication, recombination, and repair), [V] (defence mechanism), and [X] (mobilome; prophages, transposons) (Fig. S14). No unique genes were identified in *Mbv. cononymphae* among COG-assigned 911 CDSs when compared to other known *Methanobrevibacter* species (Fig. S15; Table S10). Details are described in Supplemental Results.

Predicted metabolism of *Mbv. cononymphae*

All genes for enzymes required for energy conservation through methanogenesis were present in *Mbv. cononymphae* (Fig. 5). Similar to other *Methanobrevibacter* species, it likely produces methane from H_2 and CO_2. On the other hand, the formate dehydrogenase subunit alpha gene *fdhA* is pseudogenized, and the gene for formate transporter (*fdhC*) was missing (Fig. S16). Intact *fdhA* and *fdhC* genes were not found in sequence reads outside the assembled genome or in the other eight samples that were not selected for deeper sequencing analysis. In addition, genes for the acetyl-CoA decarbonylase/synthase (ACDS) multienzyme complex were absent; thus, *Mbv. cononymphae* apparently requires acetate to produce acetyl-CoA. The cobalamin biosynthetic pathway was absent, and instead, genes for the cobalamin/siderophore transporter FepBCD were identified (Table S6). These characteristics, i.e., loss or absence of genes for Fdh, ACDS, and cobalamin biosynthesis, were shared by most MAGs derived from the guts of protist-dependent termite species, but not shared by the gut wall-dwelling species *Mbv. curvatus*, *Mbv. filiformis*, and *Mbv. cuticularis* [8, 9] (Fig. 4).

Mbv. cononymphae possesses genes for ammonium transporter AmtB and glutamine synthetase GlnA. The genome also encoded a major facilitator superfamily transporter for di- and tripeptides, which may be other nitrogen sources (Fig. 5). The amino acid and cofactor synthesis capabilities were similar to those of other *Methanobrevibacter* species (Table S11). Genes for proteins involved in oxygen tolerance, including catalase KatE, were identified (Fig. 4), and details are described in Supplemental Results. No genes related to motility were found.

Discussion

This study unveiled the ecology and genomic features of the endosymbiotic methanogen *Mbv. cononymphae* harbored by two *Cononympha* species in the gut of *C. formosanus*. A series of evidence obtained by a combination of F_{420} autofluorescence detection, small subunit (SSU) rRNA gene sequence analysis, and TEM, clearly indicated that their association is facultative and that the methanogens are most likely transmitted in "mixed mode" [62], i.e., both vertically and horizontally among *Cononympha* cells across the two *Cononympha* species. In addition, our data suggest that *Mbv. cononymphae* colonizes the hindgut wall. This facultative lifestyle is consistent with its genomic features such as the genome size comparable to those of free-living relatives, the number of pseudogenes intermediate between free-living relatives and the putatively obligate endosymbiont NOE of the anaerobic ciliate *N. ovalis* [58] (Table 1), and the presence of a catalase gene (CfCl-M3_0439, Table S6).

Catalase activity was previously observed in *Mbv. filiformis*, *Mbv. curvatus*, and *Mbv. cuticularis*, all of which attach to the microoxic hindgut wall of *R. flavipes* [8, 9]. The catalase gene *katE* was
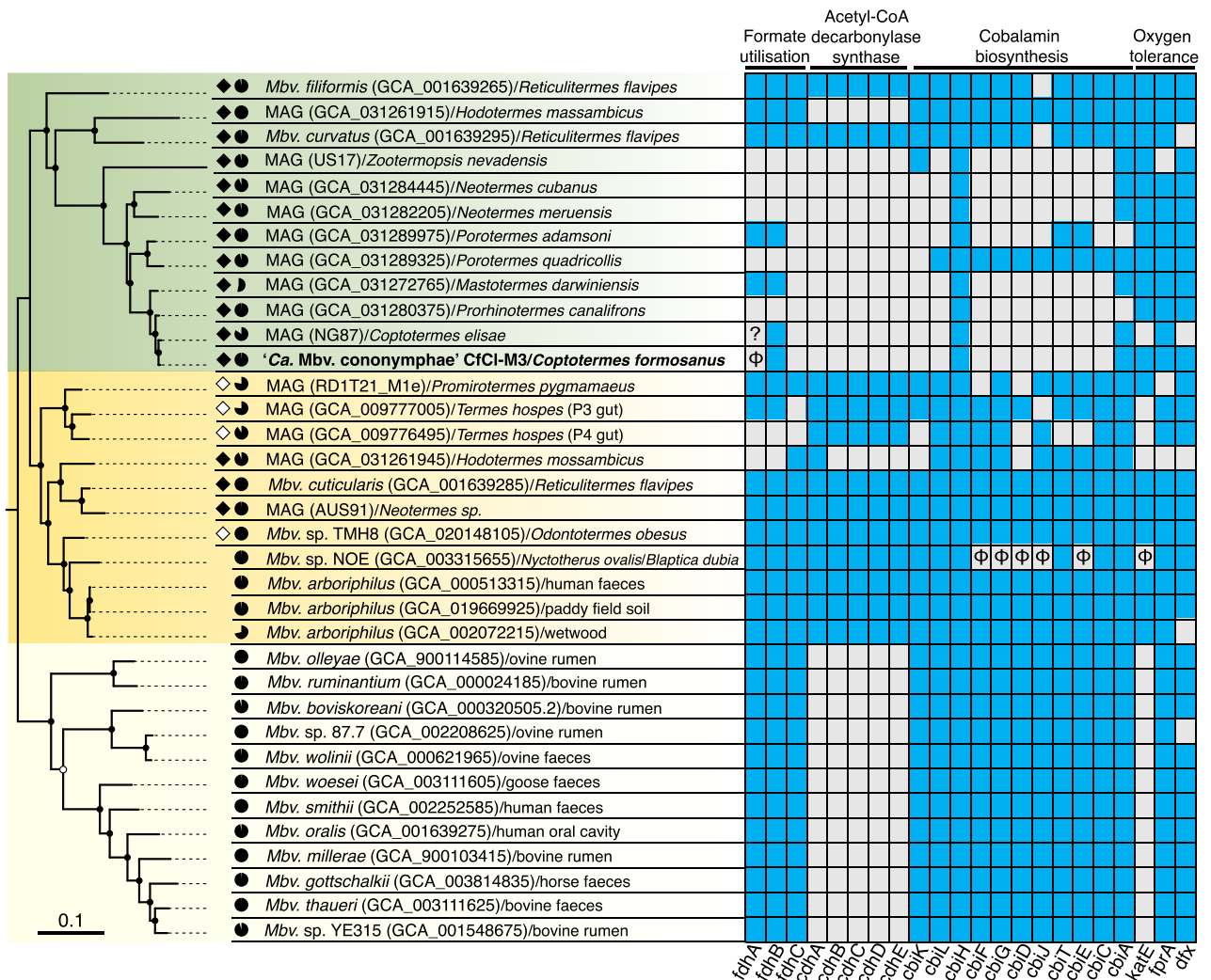
Figure 4. Phylogenetic position and characteristic genetic features of "*Ca.* Methanobrevibacter cononymphae". Maximum likelihood tree was constructed based on 42 concatenated single-copy genes using the LG + F + R5 amino acid substitution model. *Methanobacterium veterum* MK4 and *Methanobacterium bryantii* M.o.H. were used as outgroups (Table S3). Ultrafast bootstrap values of 85–95% and ≥ 95% are indicated with open and closed circles, respectively. Genomes derived from protist-dependent and protist-independent termite species are highlighted in filled and unfilled diamonds, respectively. The genome completeness estimated using CheckM is shown by pie charts. The presence or absence of genes for formate dehydrogenase FdhAB, formate transporter FdhC, acetyl-CoA decarbonylase/synthase Cdh, cobalamin biosynthesis Cbi, and oxygen tolerance (catalase KatE, $F_{420}H_2$ oxidase FprA, and desulfoferrodoxin Dfx) are linked to the phylogenetic tree. Existing and absent genes are indicated by filled (blue) and blank (grey) squares, respectively. Pseudogenes are indicated with "*φ*". The *fdhA* gene of MAG_NG87 is at a contig end and truncated; therefore, it is impossible to specify whether it is intact or pseudogenized.

commonly found in the clade containing *Mbv. cononymphae* and its sister clade; however, it is pseudogenized in *Methanobrevibacter* sp. NOE (Fig. 4). This is possibly because NOE, unlike *Mbv. cononymphae*, has become an obligate endosymbiont that rarely encounters a high concentration of oxygen.

Assuming that *Cononympha* cells produce H_2, CO_2, and acetate as the main fermentation products but do not produce formate, as observed in other cellulolytic parabasalids [63, 64] and predicted based on the transcriptome of *Cononympha* [24] (see Supplemental Methods), the loss of *fdhC* and pseudogenization of *fdhA* (Fig. S16) are likely attributable to endosymbiosis. In the hindgut of termites, the amount of formate is generally limited, but still appreciable amounts were detected [7, 65]. Indeed, the *fdh* operon is apparently intact in the genomes of the gut wall-dwelling species *Mbv. filiformis*, *Mbv. curvatus*, and *Mbv. cuticularis* (Fig. S16), even though these isolates exhibited only weak or no growth on formate [8, 9]. It is conceivable that the reduced opportunity

and/or requirement to use formate has allowed the loss of functional *fdh* genes in *Mbv. cononymphae*. The lack of ACDS in *Mbv. cononymphae* may also be related to endosymbiosis. The expectedly high concentration of acetate within the host protist cell may have allowed the endosymbiont to depend solely on acetate to produce acetyl-CoA (Fig. 5). However, as the concentration of acetate is also high in the termite hindgut [7, 65], other factors may be involved in the absence of ACDS.

The absence of the functional biosynthetic pathway of cobalamin, which is essential in methanogenesis [66] (Fig. 5), was previously reported also in the endosymbiotic methanogens *Methanobrevibacter* sp. NOE and *Methanocorpusculum* sp. MCE [58]. Thus, its absence and dependence on a transporter may be a common trait in endosymbiotic methanogens. These characteristics, i.e., the absence of functional *fdh*, ACDS genes, cobalamin biosynthetic pathway, and the presence of the catalase gene were common in most MAGs from the guts of
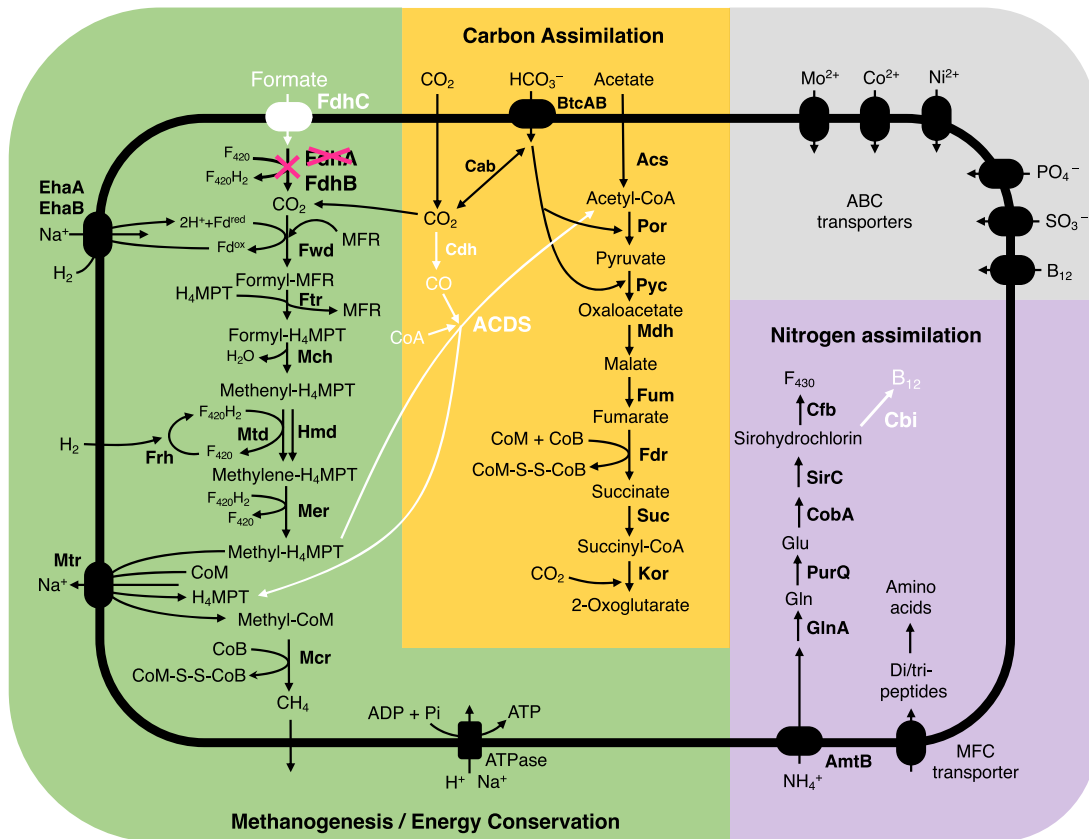
Figure 5. The predicted metabolic pathway of "*Ca.* Methanobrevibacter cononymphae." Genes or pathways characteristically absent in *Mbv. cononymphae* are shown in white. The gene for formate dehydrogenase subunit alpha (*fdhA*) is pseudogenized.

protist-dependent termites (Fig. 4). This implies that these methanogens possibly have a lifestyle similar to that of *Mbv. cononymphae*, i.e., facultative endosymbiosis, although their localizations are unidentified. Among them, MAG_NG87 from *Coptotermes elisae* [53] and MAG_GCA031280375 from *Prorhinotermes canalifrons* [5] showed high ANIs, 98.8% and 96.2%, respectively, with *Mbv. cononymphae*, and both termite genera harbour *Cononympha* species [67]; these MAGs are most likely of endosymbionts of *Cononympha* with similar lifestyles.

It is widely believed that hydrogenotrophic methanogens critically contribute to the fermentative metabolism of H_2-producing anaerobic protist hosts as syntrophic mutualists [19]. Indeed, retarded growth of anaerobic ciliates that had lost their endosymbiotic methanogens was previously observed [68, 69]. In particular, removal of "*Candidatus* Methanoregula pelomyxae", an endosymbiont of *Pelomyxa schiedti*, led to the death of the anaerobic amoeba host [70]. In the case of termite-gut protists, Messer and Lee (1989) [16] reported that *Trichomitopsis termopsidis* treated with 2-bromoethanesulfonate (BES) inhibiting methanogenesis was viable in the gut of *Z. angusticollis*. However, in an experiment using cultured *Trichomitopsis termopsidis,* the growth of the protist was severely retarded when methanogenesis was suppressed by BES treatment [64]. Its growth was recovered when fed with a more favorable nutrient source in addition to cellulose, i.e., autoclaved cells of a specific bacterial strain [64]. This reminded other reports that anaerobic ciliates during successive cultures under optimal conditions tended to lose their endosymbiotic methanogens, whereas ciliates under food-limiting conditions or at low temperatures kept housing methanogens [71, 72]. These previous results imply that the loss of *Mbv. cononymphae* may be related to the nutritional

condition of the *Cononympha* host. It is unclear whether *Mbv. cononymphae* contributes to the nutrition of the *Cononympha* host, not only by consuming H_2, but also by supplementing nitrogenous compounds as suggested in several cases of obligate endosymbioses between termite-gut protists and bacteria [12, 49, 73–75].

Although *Mbv. cononymphae* can also likely colonize the gut wall, the methane emission rate shown in Fig. 1E indicated that the absence of the endosymbiont was not compensated by methanogens outside *Cononympha* cells. Large differences in the methane emission rate among colonies were previously observed in other termite species, i.e., *R. speratus* [2]*, Neotermes sugioi* [koshunensis] [56], and *Cryptotermes secundus* [2, 7]. Thus, the facultative association of methanogens not only with gut protists but also with termite hosts may be not rare phenomena. Although what factors determine the infection rate of methanogens in gut protists and their total abundance in the termite gut remain unclear, methanogens might play a role in adjusting the fermentation process of the protist hosts and the whole termite gut ecosystem in response to changing nutritional conditions with their versatile localization and abundance.

Description of "*Candidatus* Methanobrevibacter cononymphae" sp. nov

Methanobrevibacter cononymphae (co.no.nym'phae. N.L. fem. n. *Cononymphae*, of *Cononympha,* a genus of flagellated protist hosts). The archaea are straight rods with dimensions of 1.3–1.8 μm (mean ± SD, 1.58 ± 0.1; $n = 50$) by 0.4–0.5 μm (0.4 ± 0.0). The archaea are non-motile and facultatively colonize the cytoplasm of *Cononympha leidyi* and *Cononympha koidzumii* in the gut of *Coptotermes formosanus*. The archaea occasionally colonize the

hindgut wall of *C. formosanus*. The assignment is based on the 16S rRNA gene (LC802674). The draft genome sequence CfCl-M3 showed 96.2% ANI to *Methanovirga procula,* which has been named under SeqCode on the basis of a MAG (GCA_031280375) obtained from the gut of *Prorhinotermes canalifrons* [5]. Since the genus *Methanobrevibacter* is highly divergent, Protasov et al (2023) have proposed division of *Methanobrevibacter* into at least nine genera, including *Methanovirga*, based on the genomic phylogeny and distance under SeqCode [5, 76].

Acknowledgements

Author contributions

Yuichi Hongoh and Moriya Ohkuma conceptualized the study and acquired fundings; Yuichi Hongoh, Kumiko Kihara, and Tsuyoshi Yoshimura administrated the project; Yuichi Hongoh Kumiko Kihara, Tsuyoshi Yoshimura, Masayuki Kaneko, Tatsuki Omori, and Miho Sakai-Tazawa collected termites; Tatsuki Omori, Masayuki Kaneko, Miho Sakai-Tazawa, and Katsura Igai performed experiments, Masayuki Kaneko, Tatsuki Omori, and Yuichi Hongoh analyzed and interpreted the data; Takako Mabuchi performed TEM; Arisa Nishihara, Masayuki Kaneko, and Katsura Igai measured methane; Masayuki Kaneko, Katsura Igai, and Yuichi Hongoh wrote the paper with input from the other authors.

Supplementary material

Supplementary material is available at *ISME Communications* online.

Conflicts of interest

The authors declare no competing interests.

Funding

Data availability

The 16S rRNA amplicon and metagenome sequence data generated in this study have been deposited in DDBJ under the accession numbers DRR534530–534599 (BioProject: PRJDB17265). Accession numbers for the CfCl-M3 genome are BAABUN010000001–BAABUN010000245. Representative near full-length SSU rRNA gene sequences will appear under the accession numbers LC802720–61 (18S rRNA) and LC802666–82 (16S rRNA).

References

1. Jabłoński S, Rodowicz P, Łukaszewicz M. Methanogenic archaea database containing physiological and biochemical characteristics. *Int J Syst Evol Microbiol* 2015;**65**:1360–8. https://doi.org/10.1099/ijs.0.000065

2. Sugimoto A, Inoue T, Tayasu I *et al*. Methane and hydrogen production in a termite-symbiont system. *Ecol Res* 1998;**13**:241–57. https://doi.org/10.1046/j.1440-1703.1998.00262.x

3. Brauman A, Doré J, Eggleton P *et al*. Molecular phylogenetic profiling of prokaryotic communities in guts of termites with different feeding habits. *FEMS Microbiol Ecol* 2001;**35**:27–36. https://doi.org/10.1111/j.1574-6941.2001.tb00785.x

4. Brune A. Methanogens in the digestive tract of termites. In: Hackstein JHP (ed), *Microbiology Monographs: (Endo) symbiotic Methanogenic Archaea*. Switzerland: Springer Nature, 2018, 81–101. https://doi.org/10.1007/978-3-319-98836-8_6

5. Protasov E, Nonoh JO, Kastle Silva JM *et al*. Diversity and taxonomic revision of methanogens and other archaea in the intestinal tract of terrestrial arthropods. *Front Microbiol* 2023;**14**:e1281628. https://doi.org/10.3389/fmicb.2023.1281628

6. Breznak JA, Switzer JM. Acetate synthesis from H_2 plus CO_2 by termite gut microbes. *Appl Environ Microbiol* 1986;**52**:623–30. https://doi.org/10.1128/aem.52.4.623-630.1986

7. Pester M, Brune A. Hydrogen is the central free intermediate during lignocellulose degradation by termite gut symbionts. *ISME J* 2007;**1**:551–65. https://doi.org/10.1038/ismej.2007.62

8. Leadbetter JR, Breznak JA. Physiological ecology of *Methanobrevibacter cuticularis* sp. nov. and *Methanobrevibacter curvatus* sp. nov., isolated from the hindgut of the termite *Reticulitermes flavipes*. *Appl Environ Microbiol* 1996;**62**:3620–31. https://doi.org/10.1128/aem.62.10.3620-3631.1996

9. Leadbetter JR, Crosby LD, Breznak JA. *Methanobrevibacter filiformis* sp. nov., a filamentous methanogen from termite hindguts. *Arch Microbiol* 1998;**169**:287–92. https://doi.org/10.1007/s002030050574

10. Hongoh Y, Ohkuma M. Termite gut flagellates and their methanogenic and eubacterial symbionts. In: Hackstein JHP (ed), *Microbiology Monographs: (Endo) symbiotic Methanogenic Archaea*. Switzerland: Springer Nature, 2018, 55–79. https://doi.org/10.1007/978-3-319-98836-8_5

11. Brune A. Symbiotic digestion of lignocellulose in termite guts. *Nat Rev Microbiol* 2014;**12**:168–80. https://doi.org/10.1038/nrmicro3182

12. Ohkuma M, Noda S, Hattori S *et al*. Acetogenesis from H_2 plus CO_2 and nitrogen fixation by an endosymbiotic spirochete of a termite-gut cellulolytic protist. *Proc Natl Acad Sci USA* 2015;**112**:10224–30. https://doi.org/10.1073/pnas.1423979112

13. Takeuchi M, Kuwahara H, Murakami T *et al*. Parallel reductive genome evolution in *Desulfovibrio* ectosymbionts independently acquired by *Trichonympha* protists in the termite gut. *ISME J* 2020;**14**:2288–301. https://doi.org/10.1038/s41396-020-0688-1

14. Takahashi K, Kuwahara H, Horikawa Y *et al*. Emergence of putative energy parasites within *Clostridia* revealed

by genome analysis of a novel endosymbiotic clade. *ISME J* 2023;**17**:1895–906. https://doi.org/10.1038/s41396-023-01502-0

15. Lee MJ, Schreurs PJ, Messer AC *et al.* Association of methanogenic bacteria with flagellated protozoa from a termite hindgut. *Curr Microbiol* 1987;**15**:337–41. https://doi.org/10.1007/BF01577591

16. Messer AC, Lee MJ. Effect of chemical treatments on methane emission by the hindgut microbiota in the termite *Zootermopsis angusticollis*. *Microb Ecol* 1989;**18**:275–84. https://doi.org/10.1007/BF02075814

17. Tokura M, Ohkuma M, Kudo T. Molecular phylogeny of methanogens associated with flagellated protists in the gut and with the gut epithelium of termites. *FEMS Microbiol Ecol* 2000;**33**:233–40. https://doi.org/10.1111/j.1574-6941.2000.tb00745.x

18. Hara K, Shinzato N, Oshima T *et al.* Endosymbiotic *Methanobrevibacter* species living in symbiotic protists of the termite *Reticulitermes speratus* detected by fluorescent *in situ* hybridization. *Microbes Environ* 2004;**19**:120–7. https://doi.org/10.1264/jsme2.19.120

19. Fenchel T, Finlay BJ. Free-living protozoa with endosymbiotic methanogens. In: Hackstein JHP (ed.), *Microbiology Monographs: (Endo) symbiotic Methanogenic Archaea*, 2nd edn. Switzerland: Springer Nature, 2018, 1–11.

20. Shinzato N, Takeshita K, Kamagata Y. Methanogenic and bacterial endosymbionts of free-living anaerobic ciliates. In: Hackstein JHP (ed.), *Microbiology Monographs: (Endo) symbiotic Methanogenic Archaea*. Switzerland: Springer Nature, 2018, 37–53. https://doi.org/10.1007/978-3-319-98836-8_4

21. Evans TA, Forschler BT, Grace JK. Biology of invasive termites: a worldwide review. *Annu Rev Entomol* 2013;**58**:455–74. https://doi.org/10.1146/annurev-ento-120811-153554

22. Koidzumi M. Studies on the intestinal protozoa found in the termites of Japan. *Parasitology* 1921;**13**:235–309. https://doi.org/10.1017/S0031182000012506

23. Jasso-Selles DE, De Martini F, Velenovsky JF IV *et al.* The complete protist symbiont communities of *Coptotermes formosanus* and *Coptotermes gestroi*: morphological and molecular characterization of five new species. *J Euk Microbiol* 2020;**67**:626–41. https://doi.org/10.1111/jeu.12815

24. Nishimura Y, Otagiri M, Yuki M *et al.* Division of functional roles for termite gut protists revealed by single-cell transcriptomes. *ISME J* 2020;**14**:2449–60. https://doi.org/10.1038/s41396-020-0698-z

25. Tsunoda K, Ohmura W, Yoshimura TK *et al.* Methane emission by the termite, *Coptotermes formosanus* Shiraki (Isoptera: Rhinotermitidae). *Wood Res* 1993;**79**:34–40.

26. Inoue J, Noda S, Hongoh Y *et al.* Identification of endosymbiotic methanogen and ectosymbiotic spirochetes of gut protists of the termite *Coptotermes formosanus*. *Microbes Environ* 2008;**23**:94–7. https://doi.org/10.1264/jsme2.23.94

27. Lai P, Tamashiro M, Fujii JK. Abundance and distribution of the three species of symbiotic protozoa in the hindgut of *Coptotermes formosanus* (Isoptera: Rhinotermitidae). *Proc Hawaiian Entomol Soc* 1983;**24**:271–6.

28. Yoshimura T. Contribution of the protozoan fauna to nutritional physiology of the lower termite, *Coptotermes formosanus* Shiraki (Isoptera: Rhinotermitidae). *Wood Res* 1995;**82**:68–129.

29. Trager W. The cultivation of a cellulose-digesting flagellate, *Trichomonas termopsidis*, and of certain other termite protozoa. *Biol Bull* 1934;**66**:182–90. https://doi.org/10.2307/1537331

30. Igai K, Kitade O, Fu J *et al.* Fine-scale genetic diversity and putative ecotypes of oxymonad protists coinhabiting the hindgut of *Reticulitermes speratus*. *Mol Ecol* 2022;**31**:1317–31. https://doi.org/10.1111/mec.16309

31. Murakami T, Segawa T, Dial R *et al.* Bacterial microbiota associated with the glacier ice worm is dominated by both worm-specific and glacier-derived facultative lineages. *Microbes Environ* 2017;**32**:32–9. https://doi.org/10.1264/jsme2.ME16158

32. Callahan BJ, McMurdie PJ, Rosen MJ *et al.* DADA2: high-resolution sample inference from Illumina amplicon data. *Nat Methods* 2016;**13**:581–3. https://doi.org/10.1038/nmeth.3869

33. Pruesse E, Peplies J, Glockner FO. SINA: accurate high-throughput multiple sequence alignment of ribosomal RNA genes. *Bioinformatics* 2012;**28**:1823–9. https://doi.org/10.1093/bioinformatics/bts252

34. Quast C, Pruesse E, Yilmaz P *et al.* The SILVA ribosomal RNA gene database project: improved data processing and web-based tools. *Nucleic Acids Res* 2013;**41**:D590–6.

35. Nguyen L-T, Schmidt HA, von Haeseler A *et al.* IQ-TREE: a fast and effective stochastic algorithm for estimating maximum-likelihood phylogenies. *Mol Biol Evol* 2015;**32**:268–74. https://doi.org/10.1093/molbev/msu300

36. Leigh JW, Bryant D. popart: full-feature software for haplotype network construction. *Methods Ecol Evol* 2015;**6**:1110–6. https://doi.org/10.1111/2041-210X.12410

37. Ludwig W, Strunk O, Westram R *et al.* ARB: a software environment for sequence data. *Nucleic Acids Res* 2004;**32**:1363–71. https://doi.org/10.1093/nar/gkh293

38. Utami YD, Kuwahara H, Murakami T *et al.* Phylogenetic diversity and single-cell genome analysis of 'Melainabacteria', a non-photosynthetic cyanobacterial group, in the termite gut. *Microbes Environ* 2018;**33**:50–7. https://doi.org/10.1264/jsme2.ME17137

39. Sato T, Kuwahara H, Fujita K *et al.* Intranuclear verrucomicrobial symbionts and evidence of lateral gene transfer to the host protist in the termite gut. *ISME J* 2014;**8**:1008–19. https://doi.org/10.1038/ismej.2013.222

40. Bankevich A, Nurk S, Antipov D *et al.* SPAdes: a new genome assembly algorithm and its applications to single-cell sequencing. *J Comput Biol* 2012;**19**:455–77. https://doi.org/10.1089/cmb.2012.0021

41. Lin H-H, Liao Y-C. Accurate binning of metagenomic contigs via automated clustering sequences using information of genomic signatures and marker genes. *Sci Rep* 2016;**6**:e24175. https://doi.org/10.1038/srep24175

42. von Meijenfeldt FAB, Arkhipova K, Cambuy DD *et al.* Robust taxonomic classification of uncharted microbial sequences and bins with CAT and BAT. *Genome Biol* 2019;**20**:e217. https://doi.org/10.1186/s13059-019-1817-x

43. Warren RL, Yang C, Vandervalk BP *et al.* LINKS: scalable, alignment-free scaffolding of draft genomes with long reads. *GigaScience* 2015;**4**:e35. https://doi.org/10.1186/s13742-015-0076-3

44. Xu M, Guo L, Gu S *et al.* TGS-GapCloser: a fast and accurate gap closer for large genomes with low coverage of error-prone long reads. *GigaScience* 2020;**9**:1–11. https://doi.org/10.1093/gigascience/giaa094

45. Li H. Minimap2: pairwise alignment for nucleotide sequences. *Bioinformatics* 2018;**34**:3094–100. https://doi.org/10.1093/bioinformatics/bty191

46. Tanizawa Y, Fujisawa T, Nakamura Y. DFAST: a flexible prokaryotic genome annotation pipeline for faster genome publication. *Bioinformatics* 2018;**34**:1037–9. https://doi.org/10.1093/bioinformatics/btx713

47. Couvin D, Bernheim A, Toffano-Nioche C *et al.* CRISPRCasFinder, an update of CRISPRFinder, includes a portable version,

enhanced performance and integrates search for Cas proteins. *Nucleic Acids Res* 2018;**46**:W246–51. https://doi.org/10.1093/nar/gky425

48. Tatusova T, DiCuccio M, Badretdin A *et al.* NCBI prokaryotic genome annotation pipeline. *Nucleic Acids Res* 2016;**44**:6614–24. https://doi.org/10.1093/nar/gkw569

49. Hongoh Y, Sharma VK, Prakash T *et al.* Complete genome of the uncultured Termite Group 1 bacteria in a single host protist cell. *Proc Nat Acad Sci USA* 2008;**105**:5555–60. https://doi.org/10.1073/pnas.0801389105

50. Moriya Y, Itoh M, Okuda S *et al.* KAAS: an automatic genome annotation and pathway reconstruction server. *Nucleic Acids Res* 2007;**35**:W182–5. https://doi.org/10.1093/nar/gkm321

51. Kanehisa M, Sato Y. KEGG Mapper for inferring cellular functions from protein sequences. *Protein Sci* 2020;**29**:28–35. https://doi.org/10.1002/pro.3711

52. Parks DH, Chuvochina M, Chaumeil PA *et al.* A complete domain-to-species taxonomy for Bacteria and Archaea. *Nat Biotechnol* 2020;**38**:1079–86. https://doi.org/10.1038/s41587-020-0501-8

53. Arora J, Kinjo Y, Šobotník J *et al.* The functional evolution of termite gut microbiota. *Microbiome* 2022;**10**:e78. https://doi.org/10.1186/s40168-022-01258-3

54. Rodriguez-R LM, Konstantinidis KT. The enveomics collection: a toolbox for specialized analyses of microbial genomes and metagenomes. *PeerJ* 2016;**4**:e1900v1.

55. Syberg-Olsen MJ, Garber AI, Keeling PJ *et al.* Pseudofinder: detection of pseudogenes in prokaryotic genomes. *Mol Biol Evol* 2022;**39**:msac153. https://doi.org/10.1093/molbev/msac153

56. Shinzato N, Yoshino H, Yara K. Methane production by microbial symbionts in the lower and higher termites of the Ryukyu archipelago. In: Sato S, Ishida M, Ishikawa H (eds.), *Endocytobiology V: Proceedings of the Fifth International Colloquium on Endocytobiology and Symbiosis, Kyoto, June 23–27, 1992.* Kyoto: Tübingen University Press, 1993, 161–6.

57. Miller TL. Methanobrevibacter. In: Boone DR, Castenholz RW, Carrity GM (eds.), *Bergey's Manual of Systematics Bacteriology*, 2nd edn. New York: Springer Verlag, 1989, 218–26.

58. Lind AE, Lewis WH, Spang A *et al.* Genomes of two archaeal endosymbionts show convergent adaptations to an intracellular lifestyle. *ISME J* 2018;**12**:2655–67. https://doi.org/10.1038/s41396-018-0207-9

59. Parks DH, Imelfort M, Skennerton CT *et al.* CheckM: assessing the quality of microbial genomes recovered from isolates, single cells, and metagenomes. *Genome Res* 2015;**25**:1043–55. https://doi.org/10.1101/gr.186072.114

60. Chklovski A, Parks DH, Woodcroft BJ *et al.* CheckM2: a rapid, scalable and accurate tool for assessing microbial genome quality using machine learning. *Nat Methods* 2023;**20**:1203–12. https://doi.org/10.1038/s41592-023-01940-w

61. Pourcel C, Touchon M, Villeriot N *et al.* CRISPRCasdb a successor of CRISPRdb containing CRISPR arrays and *cas* genes from complete genome sequences, and tools to download and query lists of repeats and spacers. *Nucleic Acids Res* 2020;**48**:D535–44. https://doi.org/10.1093/nar/gkz915

62. Ebert D. The epidemiology and evolution of symbionts with mixed-mode transmission. *Annu Rev Ecol Evol Syst* 2013;**44**:623–43. https://doi.org/10.1146/annurev-ecolsys-032513-100555

63. Yamin MA. Cellulose metabolism by the flagellate *Trichonympha* from a termite is independent of endosymbiotic bacteria. *Science* 1981;**211**:58–9. https://doi.org/10.1126/science.211.4477.58

64. Odelson DA, Breznak JA. Nutrition and growth characteristics of *Trichomitopsis termopsidis*, a cellulolytic protozoan from termites. *Appl Environ Microbiol* 1985;**49**:614–21. https://doi.org/10.1128/aem.49.3.614-621.1985

65. Tholen A, Brune A. Impact of oxygen on metabolic fluxes and *in situ* rates of reductive acetogenesis in the hindgut of the wood-feeding termite *Reticulitermes flavipes*. *Environ Microbiol* 2000;**2**:436–49. https://doi.org/10.1046/j.1462-2920.2000.00127.x

66. Weiss DS, Thauer RK. Methanogenesis and the unity of biochemistry. *Cell* 1993;**72**:819–22. https://doi.org/10.1016/0092-8674(93)90570-G

67. Yamin MA. Flagellates of the orders Trichomonadida Kirby, Oxymonadida Grasse, and Hypermastigida Grassi & Foa reported from lower termites (Isoptera families Mastotermitidae, Kalotermitidae, Hodotermitidae, Termopsidae, Rhinotermitidae, and Serritermitidae) and from the wood-feeding roach *Cryptocercus* (Dictyoptera: Cryptocercidae). *Sociobiology* 1979;**4**:5–119.

68. Fenchel T, Finlay BJ. Endosymbiotic methanogenic bacteria in anaerobic ciliates - significance for the growth efficiency of the host. *J Protozool* 1991;**38**:18–22. https://doi.org/10.1111/j.1550-7408.1991.tb04788.x

69. Yamada K, Kamagata Y, Nakamura K. The effect of endosymbiotic methanogens on the growth and metabolic profile of the anaerobic free-living ciliate *Trimyema compressum*. *FEMS Microbiol Lett* 1997;**149**:129–32. https://doi.org/10.1111/j.1574-6968.1997.tb10319.x

70. Treitli SC, Hanousková P, Beneš V *et al.* Hydrogenotrophic methanogenesis is the key process in the obligately syntrophic consortium of the anaerobic ameba *Pelomyxa schiedti*. *ISME J* 2023;**17**:1884–94. https://doi.org/10.1038/s41396-023-01499-6

71. Wagener S, Pfennig N. Monoxenic culture of the anaerobic ciliate *Trimyema compressum* Lackey. *Arch Microbiol* 1987;**149**:4–11. https://doi.org/10.1007/BF00423128

72. Finlay BJ, Embley TM, Fenchel T. A new polymorphic methanogen, closely related to *Methanocorpusculum parvum*, living in stable symbiosis within the anaerobic ciliate *Trimyema* sp. *J Gen Microbiol* 1993;**139**:371–8. https://doi.org/10.1099/00221287-139-2-371

73. Hongoh Y, Sharma VK, Prakash T *et al.* Genome of an endosymbiont coupling N₂ fixation to cellulolysis within protist cells in termite gut. *Science* 2008;**322**:1108–9. https://doi.org/10.1126/science.1165578

74. Ikeda-Ohtsubo W, Strassert JF, Köhler T *et al.* '*Candidatus* Adiutrix intracellularis', an endosymbiont of termite gut flagellates, is the first representative of a deep-branching clade of *Deltaproteobacteria* and a putative homoacetogen. *Environ Microbiol* 2016;**18**:2548–64. https://doi.org/10.1111/1462-2920.13234

75. Strassert JFH, Mikaelyan A, Woyke T *et al.* Genome analysis of '*Candidatus* Ancillula trichonymphae', first representative of a deep-branching clade of *Bifidobacteriales*, strengthens evidence for convergent evolution in flagellate endosymbionts. *Environ Microbiol Rep* 2016;**8**:865–73. https://doi.org/10.1111/1758-2229.12451

76. Hedlund BP, Chuvochina M, Hugenholtz P *et al.* SeqCode: a nomenclatural code for prokaryotes described from sequence data. *Nat Microbiol* 2022;**7**:1702–8. https://doi.org/10.1038/s41564-022-01214-9